The possible linkage of ENSO and IOD to JJAS rainfall variability over Ethiopia

Habtam Jenberu Wassie[1,] Tan Guirong [1,] *

[1]Key Laboratory of Meteorological Disaster, Ministry of Education (KLME)/Joint International Research Laboratory of Climate and Environment Change (ILCEC)/Collaborative Innovation Center on Forecast and Evaluation of Meteorological Disasters (CIC-FEMD), Nanjing University of Information Science and Technology, Nanjing 210044, China

*Corresponding author: tanguirong@nuist.edu.cn

Abstract

This study examined the possible linkage of ENSO and IOD to the rainfall of June to September (JJAS) over Ethiopia during 1991-2020. Liner regression and Correlation analysis are reveled the relationship between JJAS rainfall and Nino3.4 and DMI, tropical forcing mechanisms and associated circulations patterns. The results shows that JJAS rainfall is positively (negatively) correlated with Indian ocean (Pacific Ocean) sea surface temperatures (SST). Furthermore, Pacific Ocean (ENSO) events have impact on JJAS rainfall with strong negative correlation, whereas Indian ocean dipole (IOD) revealed weak positive correlation. Rainfall is largely influenced by ENSO over tropical Pacific Ocean and IOD over Indian Ocean, whereby, wet events are associated with an ascending motion of the Walker circulation on the eastern part of the Indian Ocean and western Pacific Ocean characterized by convergence at low levels and divergence at upper level. The negative anomaly in the central parts of the Pacific Ocean enhances convective activity and rising motion from the lower level, which facilitates the moisture transport to the study area and hence results in precipitation. In general, the mechanism of the variability of JJAS rainfall anomaly was associated with the variation in sea surface temperature anomaly, which depends on the forcing of the atmosphere on the Ocean and that of the Ocean on the atmosphere, especially with respect to the JJAS season (The Air-Sea interaction). The result of this study will help to improve the seasonal rainfall prediction and early warning of extreme rainfall events over Ethiopia.

Key words – Rainfall, ENSO, IOD, Circulation, Ethiopia, Correlation

1 Introduction

Rainfall variability across time and space affects all aspects of human activity, especially agricultural economies and social activities. And rainfall is the most important climate element for rainfed agriculture and the general socio-economic development of Ethiopia (Korecha and Barnston 2007; Degefu et al. 2017)). The main rain season (locally Kiremt) that covers June to September (JJAS), receives most parts of the country 65% -95% of the total annual rainfall in this season (Segele and Lamb 2005). Approximately 85% of the population is involved in rain fed agricultural activity and resulting crop production is depended on the distribution and amount of JJAS rainfall (Diro et al. 2011). Therefore, JJAS season rainfall prediction is a great importance for Agricultural activity planning and socioeconomic disaster mitigation (Segele et al. 2015 and Alhamshry et al. 2020). A good understanding of rainfall distribution and variability of the given region increases the accuracy and reliability of weather prediction, aimed at agricultural activity, saving live and minimizing the distraction of property (Ogwang et al. 2020).

The synoptic and localized system that influence rainfall of East Africa as well as Ethiopian includes Inter Tropical Convergence Zone (ITCZ), monsoon winds, subtropical high-pressure systems, easterly/westerly waves, tropical cyclones, El Nino Southern Oscillation (ENSO), Quasi Biennial Oscillation (QBO), Southern Oscillation Index (SOI) and Indian Ocean Dipole (IOD) (Alhamshry et al. 2020). Those systems are controlling the rainfall variability in amount and their distribution over the region. The inter-annual and inter-seasonal variability of rainfall over the tropics are tele-connected with the global atmosphere–ocean interaction in Indo-Pacific sector. Rainfall in Ethiopia exhibits considerable variability across in space and time. This variability is a result of complex interactions between various features acting at local and global scales.

Many documents have been done on the relation between Ethiopian rainfall and the state of ENSO and IOD. The inter-annual rainfall variability over many regions is closely related to the large-scale SST anomalies over the equatorial east Pacific (the El Niño–Southern Oscillation; ENSO) and the Indian Ocean Dipole, where warming/cooling events are associated with deficit/excess of rainfall by influencing the position of ITCZ and strength of the regional convective systems over the central and northern half of the country (Cheneka 2016; Endris et al. 2019). The findings from those studies give insight into the influence of Indian Ocean on Ethiopian JJAS rainfall. However,

most of the investigation tends to examine the possible influences and mechanisms of the contemporary events. BesideS, interdecadal abrupt changes occur in the Indian Pacific warm pool and the North Atlantic in the 1990 (Zhao et al.,2020). And the relationship between the climate over many regions and the tropical ocean also change. It is necessary to further examine the influences resulting from the ENSO and IOD. The understanding of the influence of ENSO and IOD on rainfall variability, with the associated circulation systems during the season will greatly help to improve the quality and skill of the seasonal forecast.

Hence, the main objective of this study is to check the linkage of tropical ENSO and IOD to the JJAS rainfall over Ethiopia since 1991 to 2020, and then further investigate the possible influence mechanisms of the tropical drivers. The remaining parts of this work are organized as follows: section 2 presented the Description of Study Area, section 3 contains the data and methodology, section 4 result and discussion and section 5 give the conclusion and recommendation.

2 Description of Study Area

Ethiopia is located along 3°N – 15°N latitude & 33°E – 48°E longitude in the Horne of Africa (Fig.1a), with an area of about 1.02 million square km. It is a country of geographical contrasts, varying from as much as 116 m (381 ft) below sea level in the Danakil depression to more than 4,600 m (15,000 ft) above sea level in the mountainous regions. The country ‘s topography consists of high and rugged plateaus and the peripheral lowlands. From a topographic view point, the country confines the Great African Rift Valley that bisects Ethiopia into the eastern and western escarpments. It gradually slopes up from the lowland edges of Rift Valley to the eastern and western escarpments into the southern, central, western and northern mountains. Major parts of the country are made up of a wide plateau and mountains of various heights (Fig. 1). Elevations in the country range from the 160 meters below sea level (northern exit of the Rift Valley) to over 4600 meters above sea level (of northern mountainous regions). The highest mountains are concentrated on the northern and southern plateaus of the country.

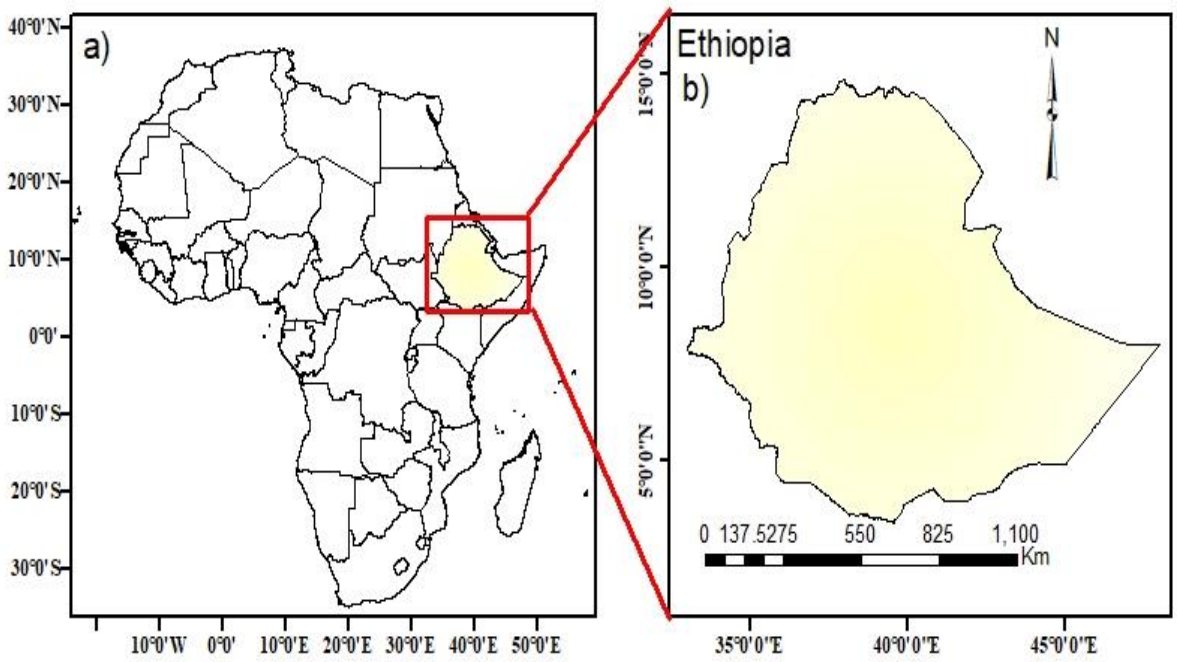

Figure 1. Study area: Map of Africa showing the area of study (shaded part) (b) Map of Ethiopia (study area)

3 Dataset and Methodology

3.1 Dataset

The monthly precipitation (rainfall) dataset used in the study obtained from remote sensing satellite estimates. Most rainfall data from in-situ meteorological stations had short period records and a large percentage of missing data problems (1991- 2020). Moreover, the spatial distributions of stations were scarce especially in the lowlands of the country. In this case, Climate Hazards Group Infra-Red Precipitation with Stations (CHIRPS) satellite rainfall data (https://data.chc.ucsb.edu/products/CHIRPS-2.0/) is a vital source of rainfall data (Asfaw et al. 2018; Dinku et al. 2018; Belay et al. 2019). CHIRPS is a quasi-global dataset (covering the area between 50° N and 50° S) available from 1981 to present-day at 0.05° spatial resolution (~ 5.3 km) and it is produced using multiple data sources (Funk et al. 2015)

Different atmospheric and oceanic indices are used as a measure of ENSO. The oceanic component of ENSO is measured by the Niño3, Niño3.4, and Niño4 SST indices over the eastern (5° N–5° S, 90°–150° W), east central (5° N–5°S, 120°–170°W), and central (5° N–5° S, 160°E–150°W)

tropical Pacific correspondingly. Monthly values of the Niño 3.4 index for the period 1991–2020 were obtained from the National Oceanic and Atmospheric Administration (NOAA) Climate Prediction Center (CPC) database(Diriba and Sorteberg 2013).

The Indian Ocean Dipole (IOD) is quantified by an index (DMI) which is obtained from the difference between SST anomalies observed between the grid boxes (50°E - 70° E, 10°S - 10° N) and (9°E - 11° E, 10° S - 0 °) as defined by (Saji and Yamagata 2003). Monthly values of DMI (1991–2020) were downloaded from the National Oceanic and Atmospheric Administration (NOAA) Climate Prediction Center (CPC) database. The monthly mean SST data sets were obtained from the National Oceanic and Atmospheric Administration (NOAA) with a 2.0° × 2.0° grid resolution for the period 1991-2020 (Japheth et al. 2021). The monthly mean Meridional and zonal winds, vertical velocity, water vapor flux, outgoing long wave radiation are obtained from the National Center for Environmental Prediction-National Center for Atmospheric Research (NCCEP-NCAR) https://psl.noaa.gov/data/gridded/data.ncep.reanalysis.pressure.html, gridded at 2.5° X 2.5° horizontal resolutions (Segele et al. 2009).

The velocity potential reflects the large-scale features of the tropical circulation and is calculated using the horizontal wind as used by Wang (2001) and Tanaka et al. (2004) following the definition;

$$\nabla v = -\nabla^2 \chi \quad \text{(1)}$$

where χ is the velocity potential anomaly, that is, a line integral of tangential wind speed along a closed circle.

And the water flux:

$$F = (1/g) \int_{Ps}^{200hPa} uqdp \quad (4)$$

Where q is the specific humidity, p_s the surface pressure, **u**= (u, v) the horizontal wind vector. For a sufficiently long period, such as a month or season

3.2 Methodology

The relationship between the JJAS Rainfall, DMI and Niño 3.4 index was computed by using simple correlation and liner regression analysis as it was used by (Endris et al. 2019; Ogwang et al. 2020). Cross-correlation is the comparison of two different time series to detect if there is a correlation between metrics with the same maximum and minimum values.

4. Results and Discussion

4.1 The Relationship between RF, IOD and ENSO

RF mainly has the interannual variation without markable decadal or trend variation (see Fig 2a). Correlation between both Dipole mode indices and Oceanic Nino indices with rainfall indices during JJAS season on 30 years was carried out in an attempt to assess the stability of linear associations between both Dipole mode indices (DMI) and Oceanic Nino indices (Nino3.4) with the rainfall (Fig2b). January DMI has largest led correlation coefficients (0.62) with the rainfall, and then during September Nino3.4 and Rainfall has closest (r = -0.66) in the period of 1991 to 2020. However, DMI has weak correlation with JJAS rainfall over the study area from March to September. And the correlation coefficients between the Nino indices before May and the rainfall are also not significant. Figure 2a also shows the interannual variation of September Nino3.4 and the January DMI. For the strong correlation between the indices, JJAS rainfall (RF) has consist variation with January Nino3.4 indices and nearly opposite variation with September DMI indices. Previous studies have also reported the same finding that ENSO or Pacific Ocean has a contribution to the variability of JJAS rainfall. However, a strong relationship is revealed when IOD events lead few months before the rainfall. While the strongest tele-connective relationship between the Oceanic Nino indices and concurrent JJAS Ethiopian seasonal rainfall is at September.

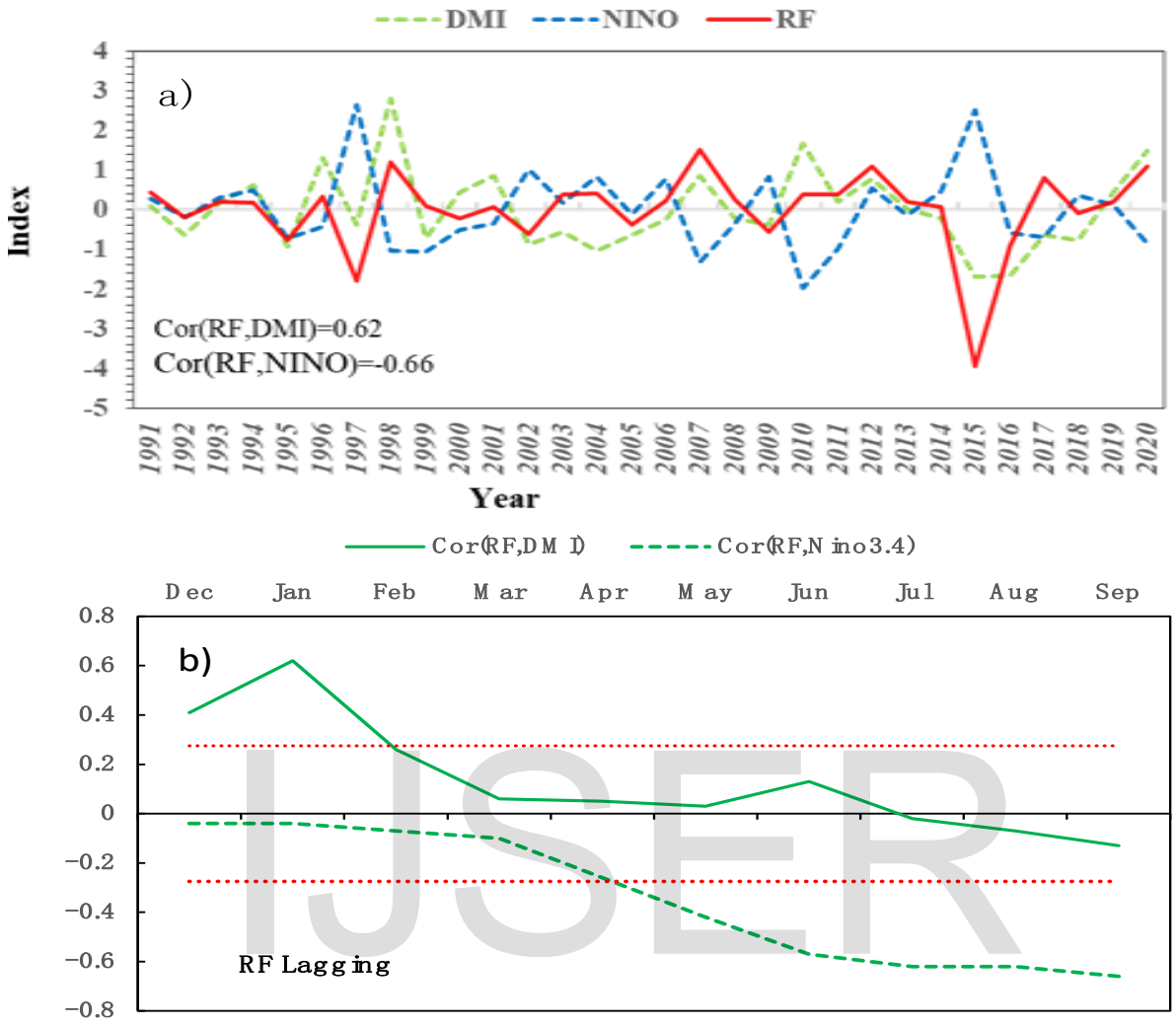

Fig 2. JJAS rainfall (mm/month) over Ethiopia, JJAS Nino3.4 and NDJ DMI index during the period 1991-2020 (a). Leading correlation coefficients (Dec to Sep) between Nino3.4, DMI and the JJAS rainfall (b). The dotted lines are values with the confidence level exceeding 95%.

4.2 Circulation Patterns Associated with JJAS rainfall

To further detect the causes of the JJAS rainfall, the associated circulation patterns are studied. The regression coefficients over the country are mostly negative on 500hPa stream function (Figure 3a), and they are negative on sea level pressure exceeding significant test of 95% (Fig 3b), revealing that when the JJAS rainfall is positive the country will be controlled by lower-than-normal pressure systems. The water transportation mainly transported by westerly flows from the west, and also by the southerly flows and northerly flows, they are convergent over the whole

country, which will be helpful for the rainfall. The negative OLR indicates strong convection. Figure 3d shows a convective zone above the western and northern Indian Ocean and western parts of the region, which is characterized by OLR lower than normal with stronger than normal convective activities. And an anomalous cyclone at 850hPa (Fig 3d) indicating convergent winds there. From the above analysis, the lower pressure systems, strong convective activity with convergent flows and water fluxes are all helpful for the formation of JJAS rainfall, and vice versa.

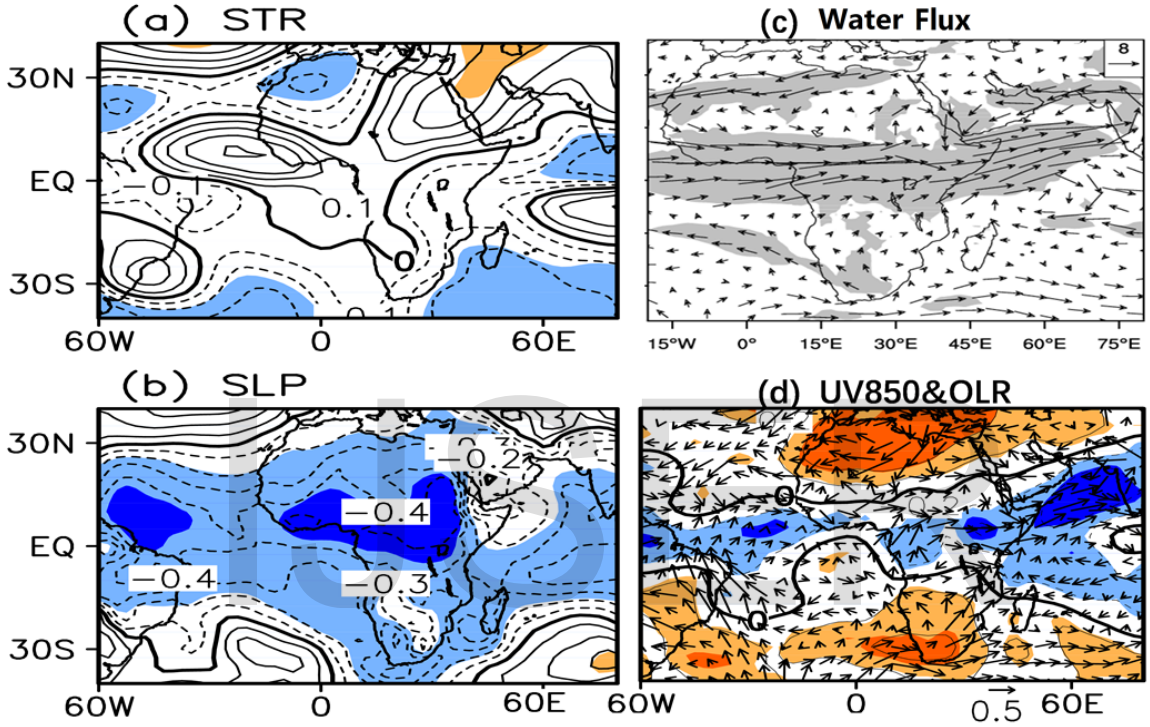

Fig 3. Regression coefficients of normalized 500hPa stream function (a), Sea level pressure(b), water flux(c), winds at 850hPa and OLR(d) on standardized JJAS rainfall anomalies averaged over Ethiopia from 1991–2020. Shaded areas with significant level at 0.05 in (a-c), but for regression coefficients of OLR in (d), with absolute values larger than 0.5 shaded.

4.3 Linkage of the JJAS rainfall to the tropical forcing

From the above analysis, the Pacific Ocean, especially the equatorial east Pacific SSTA related to Nino3.4 has significant correlation with the JJAS rainfall. The regression coefficients of the SSTA are obtained from leading Dec to September on standardized JJAS rainfall anomalies averaged over Ethiopia (see Fig. 4). The strengthening in relationship between SSTA and JJAS rainfall over the central Pacific Ocean tends to be negative (Fig. 4g to 4j), which is very significant since May. Pacific Ocean exhibited the strongest tele-connection (negative) between SST and the rainfall over

the region, due to the well-known Pacific events of ENSO. And weak relationship with western and northern Indian Ocean during JJAS season (Fig.4 i & j) for the area exceeding 95% confidence level is small, while significant positive regression coefficients can be seen on January and February. All the results are consistent with the results shown in fig2, which indicates that when the rainfall is more than normal, the SSTA in east Pacific Ocean will be negative from leading May to the JJAS season.

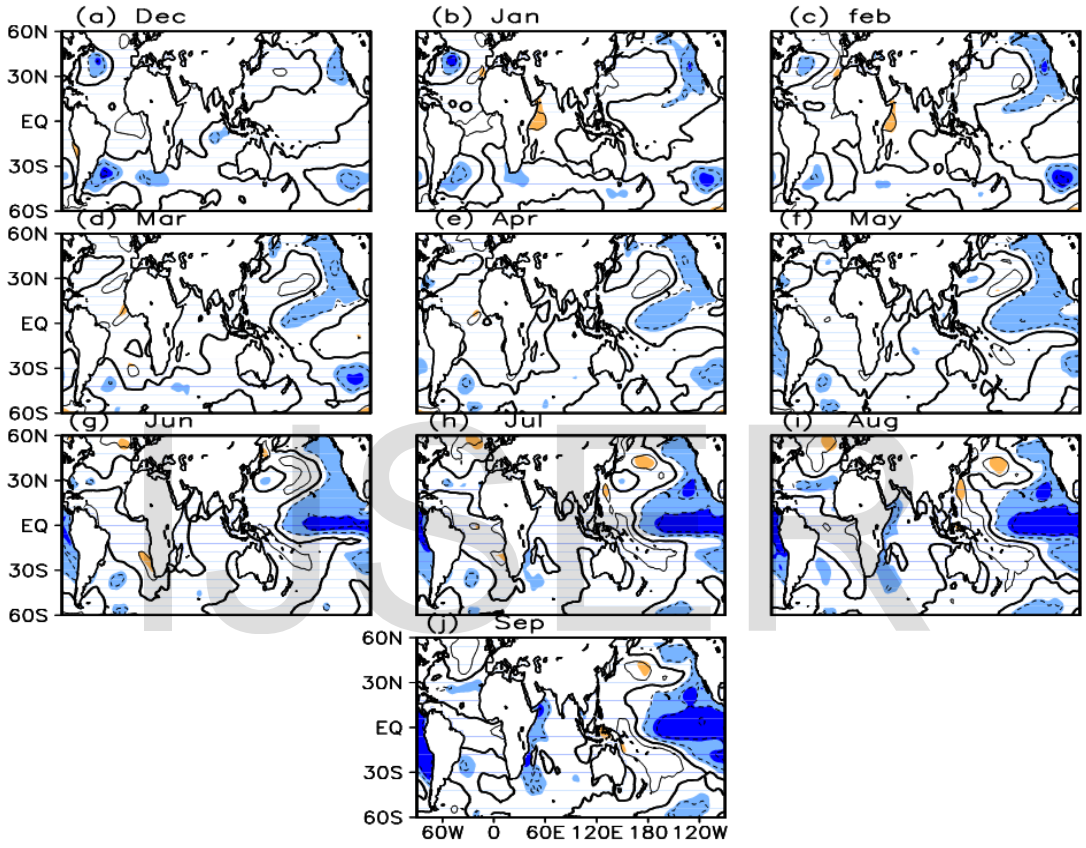

Fig 4. Regression coefficients of normalized SSTA from leading DEC to JJAS (a-j) on standardized JJAS rainfall anomalies averaged over Ethiopia during 1991–2020.Shaded areas with significant level at 0.05.

Figure5 represents Regression coefficients of normalized velocity potential at 850 hPa from leading DEC to JJAS(a-j) on standardized JJAS rainfall anomalies averaged over Ethiopia during 1991–2020. The relationship between rainfall and velocity potential are significant over the eastern Indian Ocean and western Pacific Ocean with significant level at 0.05. The results reveal that enhancing moisture from June to September are characterized by positive velocity potential anomalies and convergence at low level over the western Indian ocean and East Africa (Fig. 5g to

5j), which reposition the ascending motion over the west Pacific and easte Indian Ocean. Negative velocity potential and wind divergence at higher levels, This is completed by the descending motion in the eastern part of the Indian Ocean. This circlation pattern is clos related to the ENSO events, suppressed moisture are contrarily associated with negative values and a high centre of divergence over East Africa and Indian Ocean at low level.

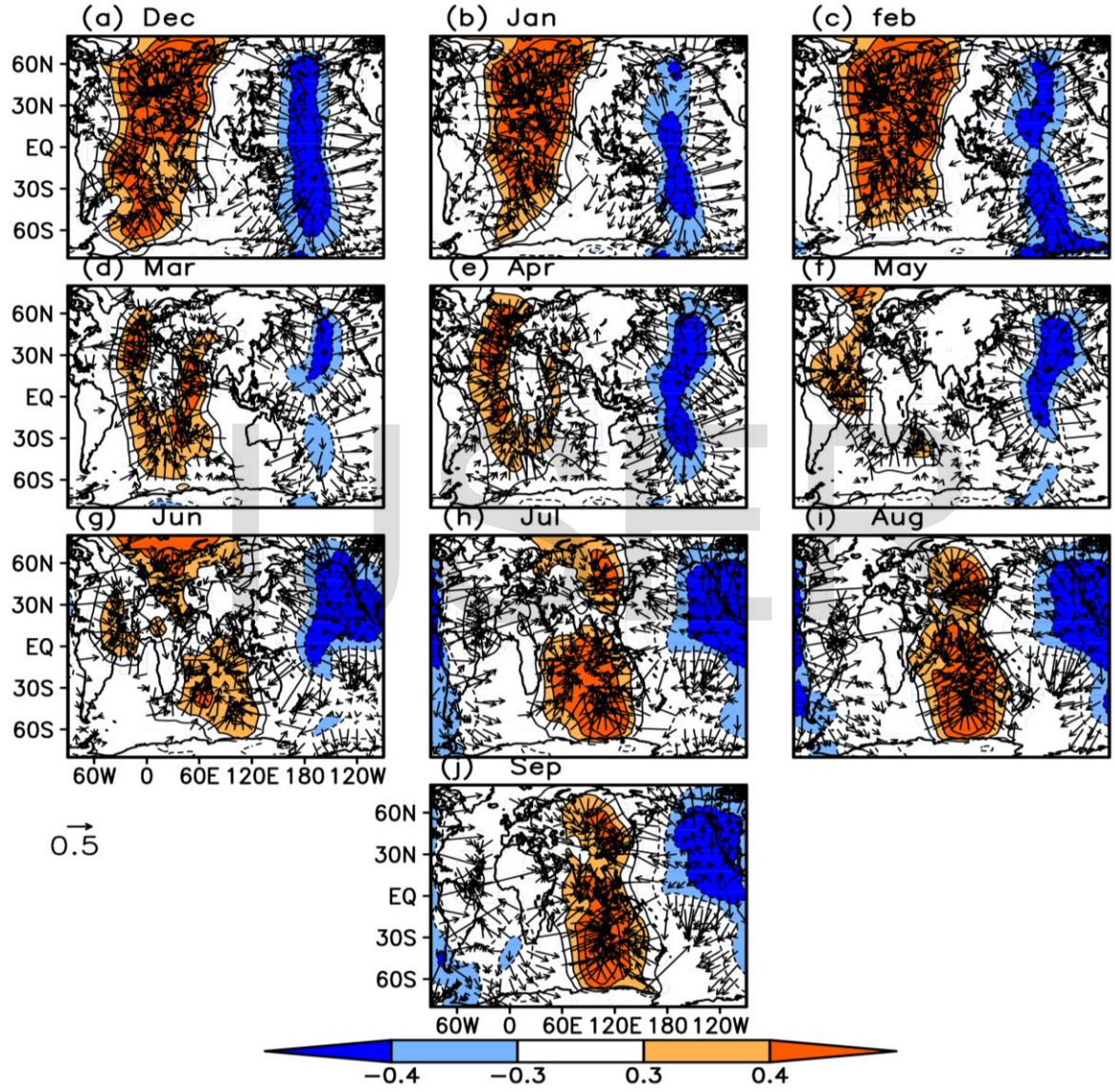

Fig 5. Regression coefficients of normalized velocity potential and divergent winds at 850 hPa from leading DEC to JJAS (a-j) on standardized JJAS rainfall anomalies averaged over Ethiopia during 1991–2020. Shaded areas show with significant level at 0.05.

4.4 Influence of the ENSO on the circulation

At 850hpa the easterly anomaly wind associated with the anticyclone flow over Arabian Sea and cyclone flow over south of Indian Ocean and there are easterly wind anomalies over Horn of Africa and Indian Ocean, and which advected moisture and make favorable for enhancement of rainfall over the study area (figure 6 a). For Ethiopia's JJAS rainy season, low level flows play vital role in transporting moisture into the country (Korecha and Barnston 2007). Negative(positive) OLR anomalies indicate enhanced (sup-pressed) convection. During JJAS of El Nino years, the zonal wave one pattern of OLR anomalies is observed along the equator, with positive OLR anomalies extending from tropical Atlantic to tropical Africa and till the Maritime Continent; negative OLR anomaly covers the equatorial Pacific (Figure 6(a)). The zonal wave one pattern can also be observed in summer of ENSO coexisting years with much weak positive OLR anomalies in tropical Africa and much intense positive OLR anomalies over the Maritime Continent. During JJAS season sea level pressure (Fig. 6b) couture indicates Mascarena High over southern Indian Ocean high-pressure system strengthens and the ridge extensions is extended and to intensify the cross-equatorial flow over the study area. These positions of rain band over the study region, and is accompanied by north westerlies and westerlies from Congo and easterlies from the southern Atlantic Ocean (Senthelina High). The negative/positive ENSO phase enhances/suppress the Mascarene high, the TEJ, and the monsoon trough more locally and the location of the low (high) sea level pressure matches with the enhanced/suppressed convection in the tropics (Cheneka 2016; Kiflie and Tao 2020) A negative anomaly of vertical wind speed (Fig. 6b) was observed from lower to upper levels between, ascending motion at low level . This is condacted by the uplifting air on mountains which favors cloud formation and hence precipitation. However, a positive vertical wind speed there is no convection at the area, which showed evidence of descending motion which cause the reduction of rainfall over the study area. At 850hpa (fig 6c), warm SSTA in the central and eastern Pacific Ocean during El Niño is accompanied by negative velocity potential anomalies aloft over the Indian Ocean region and positive anomalies over the eastern equatorial Pacific. However, 200hpa (fig6d), warm SSTs in the central and eastern Pacific during El Niño are accompanied by positive velocity potential anomalies aloft over the Indian Ocean region and negative anomalies over the eastern equatorial Pacific with significant at 95% confidence level.

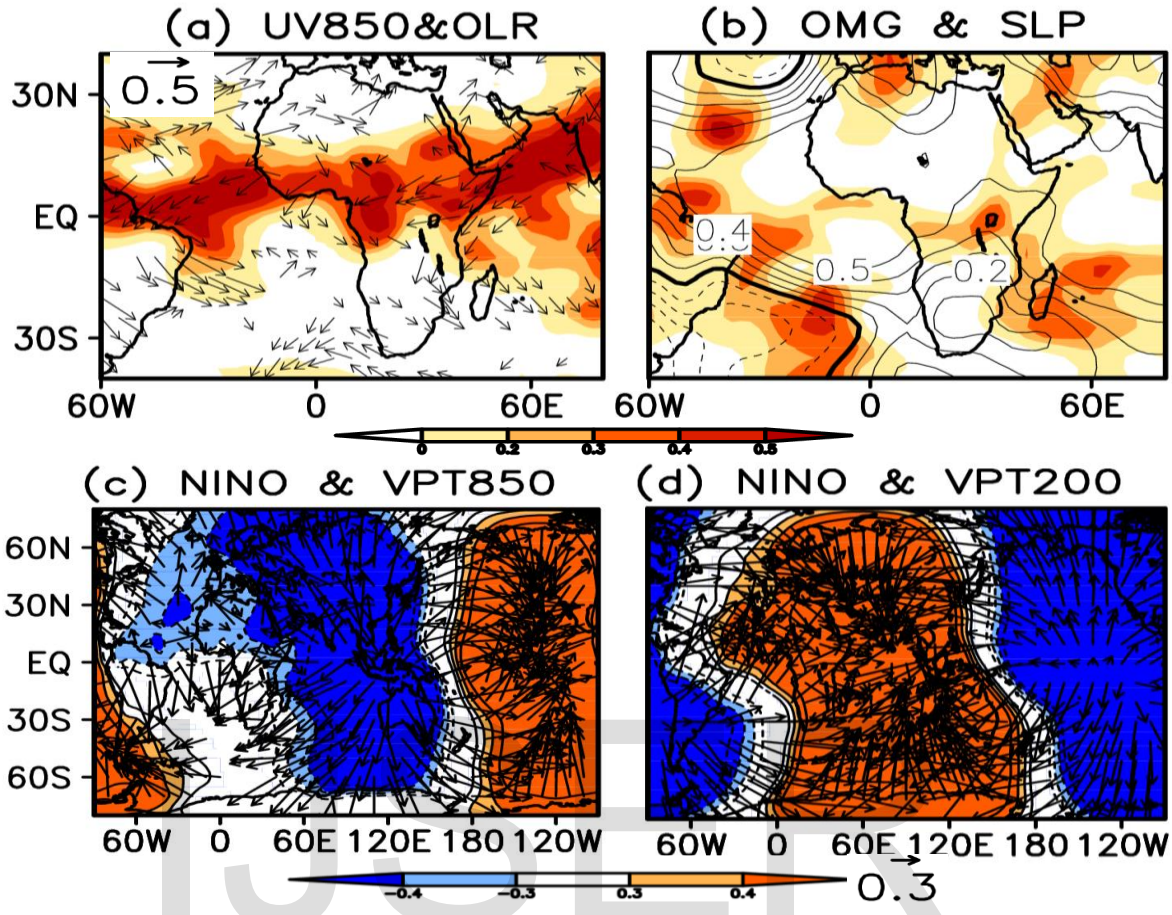

Fig 6. Regression coefficients of (a) winds at 850hPa(vectors) and OLR (shaded), (b) vertical wind speed(shaded) and SLP (contours), velocity potential at 850 hPa (c) and 200hPa (d) on Nino3.4 index. Shaded areas in (c-d) with significant level at 0.05.

5 Conclusion and Recommendation

Rainfall variability across time and space affects all aspects of human activity, especially agricultural economies and social activities. Various mechanisms have been allocated to the varying patterns of the JJAS rains. This study therefore investigated the relationship between JJAS rainfall with Nino3.4 and DMI and circulations and linkage of Tele-connection mechanisms associated with anomalous events of JJAS rainfall during the recent decades. The results JJAS rainfall and nino3.4 over the tropical Pacific Ocean tend to strong negatively correlate and DMI and rainfall weak positively correlate with correlation coefficient of -0.6 and 0.2 respectively at 95% confidence level. But, the leading correlation of DMI and rainfall is strongly with a correlation coefficient of 0. 62 and then during September Nino3.4 and Rainfall has closest relation with a correlation coefficient of -0.66. In addition, there exists a weak positive correlation of JJAS rainfall with the DMI. ENSO has more effect on rainfall over the region during JJAS than DMI. Previous studies have also reported the same finding that ENSO or Pacific Ocean has a contribution to the variability of JJAS rainfall. However, a strong relationship is revealed when there is lag in the IOD events. The negative anomaly in the central parts of the Pacific Ocean enhances convective activity and rising motion from the lower level, which facilitates the moisture transport to the study area and hence results in precipitation. This season characterized by the weakening of the Mascarene High, strong westerlies from the Congo basin at a low level and divergence of strong easterlies at the upper level. The result of this study will help to improve monitoring, prediction and early warning of extreme rainfall events over Ethiopia to reduce the vulnerability of the society to negative impacts of extreme events rainfall that are common in the area.

Acknowledgments

The author is indebted to the supervisors Prof. Tan Guirong for their consistent encouragement and guidance during the research period, and their timely review of the research and a number of manuscripts, which enabled me to come up with this final volume.

I would like to extend my appreciations to Nanjing University of Information Science and Technology, especially the staff in the college of Atmospheric science. My special thanks to Ethiopia Meteorology Institute all collogues, and also to all my classmates for the encouragement and all forms of support they rendered during my study period at the University.

Finally, I would like to thank WMO and CSC to give this chance and entire staff of Ethiopia Meteorology Institute for the support in various forms and more so, for providing the rainfall data used in the study.

References

Alhamshry A, Fenta AA, Yasuda H, et al (2020) Seasonal rainfall variability in Ethiopia and its long-term link to global sea surface temperatures. Water (Switzerland) 12:1–19. https://doi.org/10.3390/w12010055

Asfaw A, Simane B, Hassen A, Bantider A (2018) Variability and time series trend analysis of rainfall and temperature in northcentral Ethiopia: A case study in Woleka sub-basin. Weather Clim Extrem 19:29–41. https://doi.org/10.1016/j.wace.2017.12.002

Belay AS, Fenta AA, Yenehun A, et al (2019) Evaluation and application of multi-source satellite rainfall product CHIRPS to assess spatio-temporal rainfall variability on data-sparse western margins of Ethiopian highlands. Remote Sens 11:1–22. https://doi.org/10.3390/rs11222688

Cheneka BR (2016) Seasonal and Intra-Seasonal Spatial Statistical Predication of June-September Rainfall over Ethiopia Conference Inspiring and empowering women scientists / scholars for active engagement in their professional career By : Bedassa Regassa Cheneka

Degefu MA, Rowell DP, Bewket W (2017) Teleconnections between Ethiopian rainfall variability and global SSTs: observations and methods for model evaluation. Meteorol Atmos Phys 129:173–186. https://doi.org/10.1007/s00703-016-0466-9

Dinku T, Funk C, Peterson P, et al (2018) Validation of the CHIRPS satellite rainfall estimates over eastern Africa. Q J R Meteorol Soc 144:292–312. https://doi.org/10.1002/qj.3244

Diriba K, Sorteberg A (2013) Characterizing the Predictability of Seasonal Climate in Ethiopia. Water Resour Res 1–17

Diro GT, Grimes DIF, Black E (2011) Teleconnections between Ethiopian summer rainfall and sea surface temperature: Part I-observation and modelling. Clim Dyn 37:103–119. https://doi.org/10.1007/s00382-010-0837-8

Endris HS, Lennard C, Hewitson B, et al (2019) Future changes in rainfall associated with ENSO, IOD and changes in the mean state over Eastern Africa. Clim Dyn 52:2029–2053. https://doi.org/10.1007/s00382-018-4239-7

Japheth LP, Tan G, Chang'a LB, et al (2021) Assessing the Variability of Heavy Rainfall during October to December Rainfall Season in Tanzania. Atmos Clim Sci 11:267–283. https://doi.org/10.4236/acs.2021.112016

Kiflie KA, Tao L (2020) Opposite Effects of ENSO on the Rainfall over the Northern and Equatorial Great Horn of Africa and Possible Causes. Adv Meteorol 2020:. https://doi.org/10.1155/2020/9028523

Korecha D, Barnston AG (2007) Predictability of June-September rainfall in Ethiopia. Mon Weather Rev 135:628–650. https://doi.org/10.1175/MWR3304.1

Ogwang BA, Ongoma V, Shilenje ZW, et al (2020) Influence of indian ocean dipole on rainfall variability and extremes over southern africa. Mausam 71:637–648

Saji NH, Yamagata T (2003) Possible impacts of Indian Ocean Dipole mode events on global climate. Clim Res 25:151–169. https://doi.org/10.3354/cr025151

Segele ZT, Lamb PJ (2005) Characterization and variability of Kiremt rainy season over Ethiopia. Meteorol Atmos Phys 89:153–180. https://doi.org/10.1007/s00703-005-0127-x

Segele ZT, Lamb PJ, Leslie LM (2009) Seasonal-to-interannual variability of Ethiopia/horn of Africa monsoon. Part I: Associations of wavelet-filtered large-scale atmospheric circulation and global sea surface temperature. J Clim 22:3396–3421. https://doi.org/10.1175/2008JCLI2859.1

Segele ZT, Richman MB, Leslie LM, Lamb PJ (2015) Seasonal-to-interannual variability of ethiopia/horn of Africa monsoon. Part II: Statistical multimodel ensemble rainfall predictions. J Clim 28:3511–3536. https://doi.org/10.1175/JCLI-D-14-00476.1

Tanaka, H. L., N. Ishizaki and AK (2004) Trend and interannual variability of Walker, monsoon and Hadley circulations defined by velocity potential in the upper troposphere. Tellus 56A:250–269

Wang C (2001) Atlantic Climate Variability and Its Associated Atmospheric Circulation Cells. J Clim 15:1516–1536. https://doi.org/10.1175/1520-0442(2002)015<1516:ACVAIA>2.0.CO;2